Journal of Thermal Analysis and Calorimetry, Vol. 90 (2007) 2, 611–621

Review Paper

INTERMEDIATE STATES OF MYOSIN HEAD DURING ATP HYDROLYSIS CYCLE IN PSOAS MUSCLE FIBRES BY EPR AND DSC
A review

D. Lőrinczy[*] *and J. Belágyi*

Institute of Biophysics, Faculty of Medicine, University of Pécs, H-7624 Pécs, Szigeti str. 12, Hungary

Force generation in muscle during contraction arises from direct interaction of the two main protein components of the muscle, myosin and actin. The process is driven by the energy liberated from the hydrolysis of ATP. In the presence of CaATP the energy released from hydrolysis produces conformational changes in myosin and actin, which can be manifested as an internal motion of myosin head while bound to actin. It is suggested that myosin heads attached to actin produce conformational changes during the hydrolysis process of ATP, which results in a strain in the head portion of myosin in an ATP-dependent manner. These structural changes lead to a large rotation of myosin neck region relieving the strain.

Paramagnetic probes and EPR spectroscopy provide direct method in which the rotation and orientation of specifically labelled proteins can be followed during muscle activity. In order to find correlation between local and global structural changes in the intermediate states of the ATPase cycle, the spectroscopic measurements were combined with DSC measurements that report domain stability and interactions.

In the review a detailed description of the application of EPR and DSC techniques in muscle protein research will be given. The measurements show that the small local structural changes detected by EPR after nucleotide binding influence the global structure of protein system responsible for muscle contraction.

Keywords: *DSC, EPR, intermediate states of ATP hydrolysis, muscle fibre*

Introduction

The force generation in muscle during contraction arises from direct interaction of the two main protein components of the muscle, myosin and actin. The process is driven by the energy liberated from the hydrolysis of ATP. The energy released from hydrolysis produces conformational changes in myosin and/or in actin, which can be manifested as an internal motion of myosin head while bound to actin [1–9]. During the cyclic interaction of myosin (M) with ATP and actin (A) at least six intermediates are proposed for actomyosin ATPase in solution [10]. The main goal of the recent efforts is the investigation of energetic of the actomyosin ATPase in different intermediates of the contractile cycle. The better understanding of the interrelation between the thermodynamic changes observed in protein solutions in the intermediate states of the ATP hydrolysis and the mechanical activities on cellular level requires experiments on supramolecular complexes where stabilising forces may modulate the hydrolysis process.

EPR is one of the spectroscopic tools, similar to optical absorption, IR, CD, which has its range of applications and limitations. A basic biological problem cannot solve with EPR alone, but more often it can contribute to a solution as an adjunct to other methods. Most molecules have paired up electronic spins and are diamagnetic; therefore paramagnetic molecules are required as probe molecules to monitor the structure and the behaviour of the biomolecules. The spin-labeling technique was introduced about forty years ago by McConnell *et al.* [11]. The analysis of the EPR spectra of the labeled proteins allows deriving the degree of mobility and the conformational changes brought about by some biochemical process [12, 13]. Using this technique, we summarize our efforts and results obtained in study of striated muscle fibres in different states of ATP hydrolysis.

* Author for correspondence: denes.lorinczy@aok.pte.hu

1388–6150/$20.00

Akadémiai Kiadó, Budapest, Hungary
Springer, Dordrecht, The Netherlands

The powerful DSC technique allows the derivation of heat capacity of proteins as a function of temperature. From the deconvolution of the thermal unfolding patterns it is possible to characterize the structural domains of the macromolecules [14–16]. We try to approach the temperature-induced unfolding processes in different intermediate state of ATP hydrolysis in striated muscle fibres. We have extended the experiments to study the fibre system prepared from psoas muscle of rabbit in rigor, strongly binding and weakly binding states of myosin to actin where the inorganic phosphate (P_i) was substituted by the phosphate analogue orthovanadate, AlF_4^- and BeF_X^- [17].

Experimental

Materials and methods

Fibre preparation

Glycerol-extracted muscle fibre bundles were prepared from rabbit psoas muscle by standard methods [18]. ATPase activity of fibres was determined using the pyruvate kinase-lactate dehydrogenase coupled optical test [19, 20]. Mg^{2+}-ATPase activity (μmol of P_i/mg myosin min) was 4.131±0.718 μmol of P_i/mg myosin min (n=4), whereas ATPase activity of active fibre bundles was 5.565±0.816 μmol of P_i /mg myosin min (n=4).

Spin-labelling

Spin-labelling of fibres was performed in rigor solution (80 mM potassium propionate (KPr), 5 mM $MgCl_2$, 1 mM EGTA in 20 mM MOPS buffer, pH 7.0) plus 2 mM pyrophosphate at pH 6.5) with about two moles of TCSL to one mole myosin for 20 min at 0°C. Before spin-labelling, the fibres were incubated in low ionic strength buffer (1 mM EGTA, 5 mM $MgCl_2$, 1 mM DTNB and 20 mM MOPS, pH 7.5) for 1 h to achieve selective labelling of the reactive thiols [21]. The ratio of the attached spin labels to mole of myosin varied between 0.22–0.41 (mean value 0.33) as calculated from the double integral of the EPR spectra after comparison with the double integral of an MSL solution of 10 μM using the same sample cell and spectrometer parameters.

EPR measurements

Conventional and ST EPR spectra were taken with an ESP 300E (Bruker, Germany) spectrometer. First harmonic, in-phase, absorption spectra were obtained by using 20 mW microwave power and 100 kHz field modulations with amplitude of 0.1 or 0.2 mT. Second harmonic, 90° out-of-phase, absorption spectra were recorded with 63 mW and 50 kHz field modulation of 0.5 mT amplitude, detecting the signals at 100 kHz out-of-phase. The 63 mW microwave power corresponds to average microwave field amplitude of 0.025 mT in the centre region of the standard tissue cell of Zeiss (Carl Zeiss, Germany), and the values were obtained by using the standard protocol of Fajer and Marsh [22]. In order to perform precise phase setting for ST EPR technique, a different procedure was applied [23]. The idea of the method originates from B. H. Robinson (Department of Chemistry, Nashville University). Adopting the assumption that at low microwave power the variance of the EPR signal should be minimum over the whole field scan at out-of-phase setting, a proper phase angle can be calculated from two high-power spectra differing in phase angle exactly by 90°. Comparison of the results with the low-power phase setting and integral methods [24, 25] showed that this procedure – called variance method – was nearly equivalent to the other ones and had an outstanding stability.

Calorimetric measurements

The thermal unfolding of muscle fibres in different states were monitored by a SETARAM Micro DSC-II calorimeter. All experiments were done between 0 and 100°C. 0.3–0.5 K min^{-1} was used as a scan rate. Conventional Hastelloy batch vessels were used during denaturation experiments with 850 μL sample volume in average. Rigor buffer was used as reference sample. The sample and reference vessels were equilibrated with a precision of ±0.1 mg. There was no need to do any correction from the point of view of heat capacity between the sample and reference vessels. The Setaram two-point fitting integration software was used to calculate the calorimetric enthalpy.

Results and discussion

Application of EPR in myosin motor dynamics

Muscle contraction and other events of cell motility are based on the cyclic interaction of the head portion of myosin with actin during the myosin-catalysed ATP hydrolysis (Fig. 1). The hydrolysis induces conformational changes in the environment of the labelled site, it is expected that the EPR spectra exhibit differences in line shape (Fig. 2). The ATP hydrolysis that produces the AM**·ADP·P_i complex (A denotes actin and M stands for myosin) and the protein-bound ADP and P_i is a rapid process; therefore special biochemical procedures are required to follow the elementary steps of the cleavage, and to obtain detailed information about the conformational changes of the

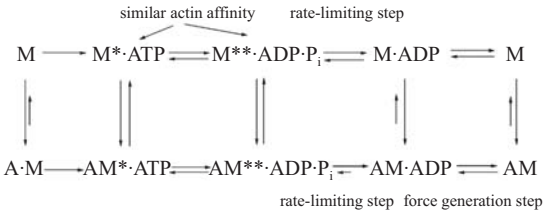

Fig. 1 Actomyosin ATPase scheme. Horizontal arrows show the transitions between the different nucleotide binding states, whereas the vertical lines represent the dissociated complexes. Starred M* and M** are intermediates of myosin in the hydrolysis cycle

interacting proteins. It was found by Goodno [26] that a complex of myosin with ADP and orthovanadate formed a stable structure. The tightly binding P_i analogue orthovanadate (V_i) has allowed study of these initial states in relative isolation from the reminder of the hydrolysis cycle. Similar to vanadate, beryllium and aluminium fluorides also form stable complexes with myosin in the presence of nucleotides [27, 28]. It turned out that the stable complexes of ADP with vanadate; beryllofluoride and aluminofluoride bound to head of myosin mimic quite well the ATPase intermediates [29].

Internal dynamics of myosin head in fibres

Strong binding state of myosin to actin (rigor, ADP)

The spin labels in fibres were immobilized on the microsecond time scale, and rotated with an effective rotational correlation time of 60 μs in the absence of nucleotides calculated from ST EPR spectra (Fig. 3). The maleimide (MSL) and isothiocyanate (TCSL) probes provided direct information about the orientation of myosin heads; in rigor the myosin heads had only one mode of binding [12, 13]. MSL probes showed a narrow distribution with respect to the longer axis of the fibres with a mean angle of 82° and an angular spread of 6°. Using TCSL probes, the EPR spectra also reported a high dependence of orientation [30], but in comparison

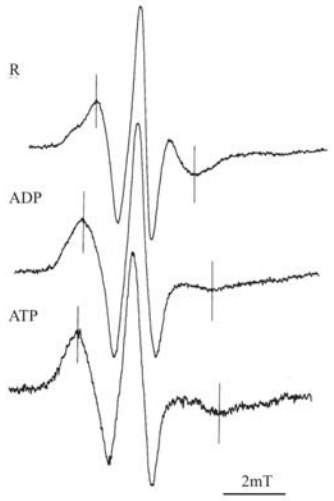

Fig. 2 Conventional EPR spectra of TCSL-fibres isolated from rabbit skeletal psoas muscle in different states of the ATP hydrolysis. MgADP or MgATP was added in 5 mM concentration to rigor buffer before EPR measurements. The distance between the outermost hyperfine extrema is characteristic of different nucleotide binding state. The spectra were taken in parallel orientations of fibres with respect to the laboratory magnetic field. The field scan was 10 mT

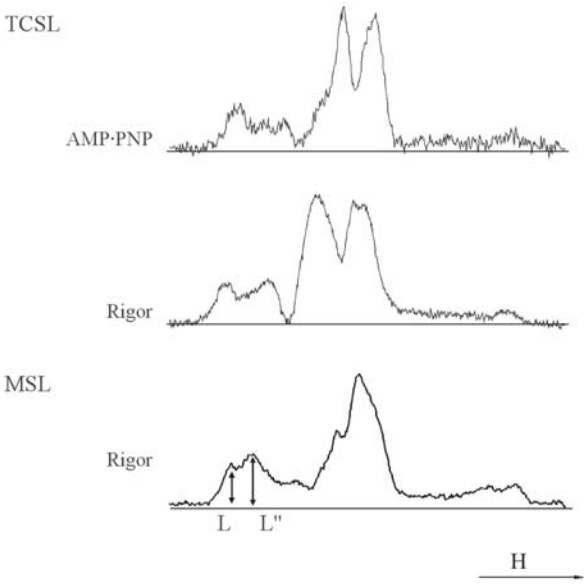

Fig. 3 Saturation transfer EPR spectra of MSL- and TCSL-fibres. The lower L''/L value of TCSL-fibres in rigor is the sign of a decreased rotational correlation time. The uppermost spectrum was obtained on TCSL-fibres in AMP·PNP state. 16 mM AMP·PNP was added to the rigor buffer, and after 10 min incubation the spectrum was recorded. The spectra were taken in perpendicular orientations of fibres with respect to the laboratory magnetic field. The field scan was 10 mT

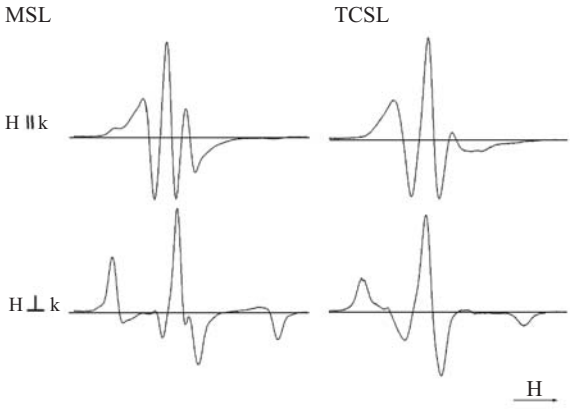

Fig. 4 Conventional EPR spectra of MSL- and TCSL-fibres in rigor. The longer axis of fibres was oriented parallel and perpendicular to the laboratory magnetic field. The field scan was 10 mT

to MSL-fibres with different mean angle and larger angular spread (ϑ=75°, σ=16°, Fig. 4).

In the presence of nucleotides (ADP) the conventional EPR spectra showed large changes in the distribution of TCSL probe molecules in fibres. Addition of 5 mM MgADP to buffer resulted in a change in the mean angle of the distribution of spin labels (Fig. 5). It decreased from 75 to 56° and the angular spread increased by four degrees, but the orientation order remained preserved. Using MSL probes, only a very small change was detected in spectra of MSL-fibres. It seems that TCSL probe molecules have favourable orientation with respect to the long axis of fibres. The flexibility of the motor domain detected between Cys 707 and Lys 553 changed only slightly after ADP binding. This support the view that the specific binding of ADP to myosin produces only small conformational change in the environment of the nucleotide-binding site, and this does not lead to overall dynamic change of the motor domain. Binding of MgADP produces neither change in the stereo specific binding of myosin head to actin nor any modification in internal motion of the actomyosin complex. It seems TCSL probe can distinguish between the two strong binding states of myosin to actin. Precise measurements made on muscle fibres with the use of ^{15}N and deuterized maleimide spin labels and sophisticated spectral analysis gave evidence that even in the case of maleimide spin label small conformational changes were produced on myosin, following nucleotide binding to myosin [31].

Week binding state of myosin to actin

The nonhydrolyzable analogue of ATP AMP·PNP, produced a random population of myosin heads, which was superimposed on rigor or ADP-like spectrum (Fig. 6). In agreement with former data the fraction of the ordered population was estimated to be approximately 50% of the total spin concentration [32]. One component of the spectra of MSL-fibres reflected exactly the same orientation as in rigor; seemingly the myosin heads remained bound to actin in the same conformation. The second component was characteristic of randomly oriented myosin heads. In the case of TCSL-fibres the component of the spectrum with high degree of order was the same as in ADP-state, the second component represented the disordered heads. The ratio of the double integrals of the component spectra was about 50:50 %. It supports the view that in the presence of nonhydrolyzable nucleotide analogue the ordered population reflects an ADP-state, and not a rigor [33]. It is known from EPR studies that the addition of MgATP plus orthovanadate to rigor solution produces large conformational changes in muscle fibres, only one spectral component can be detected, which is characteristic of a random population of spin labels [34]. The digital subtraction of the ATP·V_i-spectrum from the spectrum of TCSL-fibres in AMP·PNP-state resulted in a spectrum similar to that of TCSL-fibres in ADP-state.

The comparison of EPR spectra obtained on homogenized fibres in rigor and AMP·PNP-state showed significant decrease of rotational mobility. ST-EPR spectra of TCSL-fibres in the presence of AMP·PNP showed also changes in the rotational mobility (Fig. 3). The ratio of the low-field diagnostic peaks L''/L changed from 0.800±0.064 (n=5) to 0.675±0.094 (n=3).

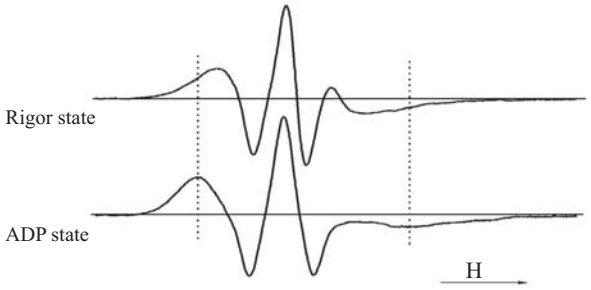

Fig. 5 Conventional EPR spectra of TCSL-fibres in rigor and ADP-state. The spectra were taken in parallel orientation. The fibres were kept in buffer solution during spectrum accumulation. MgADP was added in 5 mM concentration and the fibres were kept for 10 min before EPR measurements. The change of the hyperfine splitting ($2A'_{zz}$) shows the different distribution of spin labels in rigor and ADP-state. The field scan was 10 mT

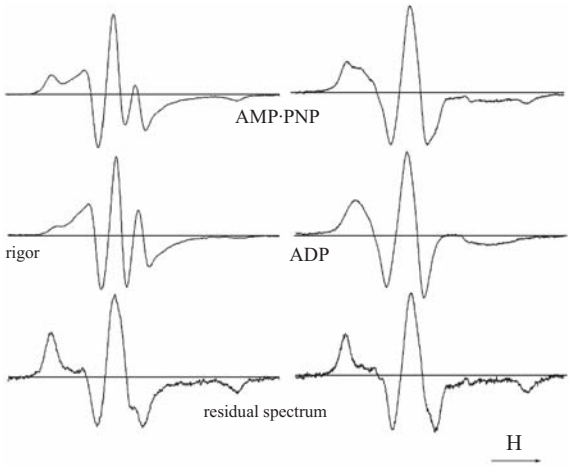

Fig. 6 Conventional EPR spectra of MSL (left) – and TCSL-fibres (right) in AMP·PNP-state. The longer axis of fibres was oriented parallel to the laboratory magnetic field. Digital subtraction of the rigor and ADP spectrum from the AMP·PNP spectrum resulted in a spectrum (difference spectrum), which was characteristic of randomly oriented spin labels. Bottom: the residual spectra. The field scan was 10 mT

It is known from literature that the AM**·ADP·P_i complex is the predominant intermediate of the ATP hydrolysis cycle in myosin and actomyosin system [35–37]. In isolated form of myosin the half-life is only a few seconds at 25°C, therefore further stabilization is needed in muscle fibres to perform detailed structural or dynamic analysis of this transition state. It was shown by Goodno that orthovanadate inhibits the myosin ATPase activity by formation a long-lived M**·ADP·V_i complex [26]. This complex is similar to M**·ADP·P_i state, and the inhibition can be reversed by dialysis. This experimental result opened the possibility to examine a stable myosin-nucleotide product by EPR and other spectroscopic technique. It turned out that in fibre study the EPR spectrum has no orientation dependence (Fig. 7). The myosin head disorder is due to dissociation of heads from actin or to a conformational change leading to non-specific week binding of myosin to actin. But this week binding does not produce large effect on the overall conformation of myosin head. Addition of ADP and V_i to the muscle sample in rigor state led to a partial relaxation, according to Danzig and Goldman vanadate forms stable complex with ADP only in the case when V_i added with ATP together [38].

Similar to vanadate, beryllium and aluminium fluorides also form stable complexes with myosin in the presence of nucleotides [27–29, 39]. These compounds are in many ways similar to vanadate that was derived from fluorescence measurements. The tight binding of AlF_4^- and BeF_X^- is accompanied by the entrapment of equistoichiometric amount of ADP, which suggests that both compounds are bound to the same site as the anionic form of P_i. They are located close to the β-phosphate group. Recent data indicate that the M·ADP·BeF_X^- complex is different from ADP·vanadate and ADP·AlF_4^- [8]. The crystal structure of *Dictyostelium* myosin looks similar to chicken myosin without nucleotides, while other complexes exhibited small changes in the head of myosin [40]. The different results between the ATP-like complexes did not result from large movement of a single domain rather than from small change in the protein structure. The ADP·BeF_X^- state is thought to be an analogue for M·ATP, whereas ADP·AlF_4^- and ADP·V_i states are analogues of the transition state.

In fibre studies, almost no or small orientation dependence was detected in the presence of ATP and beryllium or aluminium fluoride (Fig. 8). The myosin heads represented disordered populations with reduced rate of rotational motion, characterizing of dissociated myosin heads or non-specific binding of myosin heads to actin. The spectrum of ADP·BeF_X^- complex seemed to be the superposition of an ADP·V_i-like spectrum and the spectrum of a protein moiety which rotated with an effective rotational correlation time of 15 ns (Fig. 9). Digital subtraction of either an ADP·V_i spectrum or an ADP·AlF_4^- spectrum from the ADP·BeF_X^- spectrum resulted in two frac-

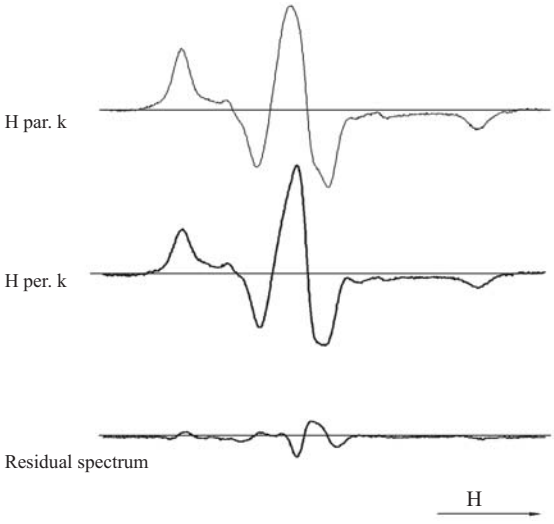

Fig. 7 Conventional EPR spectra of TCSL-fibres in M**ADP·V_i -state. The longer axis of fibres was oriented parallel and perpendicular to the laboratory magnetic field. ATP and orthovanadate were added in 5 mM concentration to rigor buffer and the fibres were kept for 10 min before EPR measurements. Bottom: residual spectrum after digital subtraction

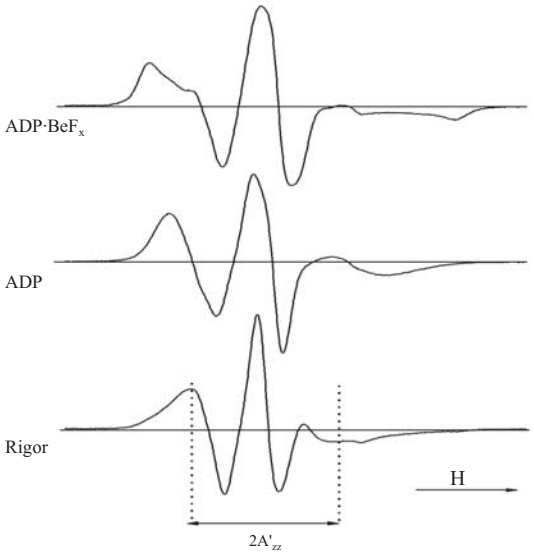

Fig. 8 Conventional EPR spectra of TCSL-treated fibres in ATP·BeF_X^-, ADP and rigor states. The longer axis of fibres was oriented parallel to the laboratory magnetic field. The fibres were treated with 5 mM MgATP and BeF_X^-. Beryllium fluoride was prepared from 10 mM NaF and 3 mM $BeSO_4$ immediately before experiments. Muscle fibres were stored in rigor solution plus the corresponding chemicals for 15 min at 0°C and then measurement was taken

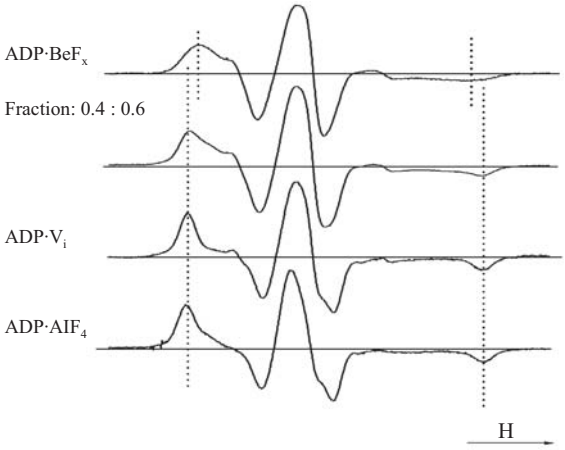

Fig. 9 Decomposition of the ATP·BeF_X^- spectrum into two components. The ATP·AlF_4^- or the ADP·V_i spectrum was subtracted from the ATP·BeF_X^- spectrum (spectrum in the second line). The difference spectrum (first line) has a rotational correlation time of about 15 ns

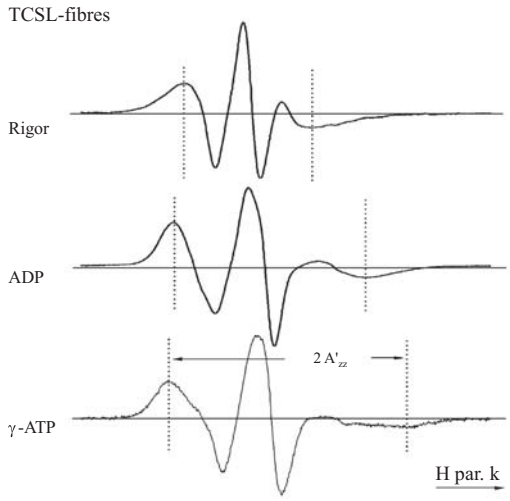

Fig. 10 Conventional EPR spectra of TCSL-fibres in rigor, ADP- and ATP[γS] states. The spectra were taken in parallel orientation. The fibres were kept in buffer solution during spectrum accumulation. Magnesium and ATP[γS] were added in 5 mM concentration and the fibres were kept for 10 min before EPR measurements. The change of the hyperfine splitting ($2A'_{zz}$) shows the different distribution of spin labels in rigor, ADP and ATP[γS] state. The field scan was 10 mT

tions with a ratio of 2 to 3. This result suggests that under experimental conditions two conformers existed in ADP·BeF_X^- state, mimicking the M*·ATP and M**·ADP·P_i states.

The slowly hydrolysed ATP analogue adenosine 5'-(γ-thiotriphosphate) (ATP[γS]) has been used in many studies of motor protein myosin in order to form a stable week ternary complex. ATP[γS] is hydrolysed by myosin at a steady state that is comparable to the intrinsic non-actin-activated steady state hydrolysis for ATP. Brenner *et al.* showed that cross-bridges in the presence of ATP[γS] have the properties of the week binding states of ATP hydrolysis cycle; but the rate constants of cross-bridge dissociation from actin reduced by a factor of about 2 order of magnitude [41, 42]. EPR spectra of TCSL-fibres are shown in Fig. 10 in different states of ATP hydrolysis. In the presence of ATP[γS] the orientation order was significantly reduced; only small orientation dependence could be detected. Using digital subtraction, almost the same spectrum was detected in both orientations of fibres, evidencing the week binding of myosin in the presence of ATP[γS].

It is interesting to note that the spectrum in the presence of ATP[γS] is almost identical with the spectrum obtained in ADP·BeF_X^- state (see spectrum in the first line in Fig. 9). Fischer *et al.*, later Geeves and Holmes have shown that ADP·BeF_X^- state mimics the myosin·ATP state [4, 8]. It cannot be excluded that the near identity of the EPR spectra obtained in the presence of ADP·BeF_X^- state and ATP[γS] represent the same event. The results of ADP·BeF_X^- state suggest that this state is heterogeneous, the superposition of the intermediate states M*·ATP and AM^{**}·ADP·P_i. In contrast the ADP·AlF_4^- state cannot be distinguished from the ADP·P_i (AM**·ADP·V_i) state. Accordingly, our experiments are in accordance with the view that during ATP hydrolysis the myosin head goes from a non-specific weakly binding state to a highly specific strongly binding state that generates tension and the conformational changes of myosin during the consecutive steps of the ATP hydrolysis reflects functionally relevant conformational changes.

DSC measurements on fibre systems

Evaluation of thermal transitions

The DSC transitions of muscle fibres exhibited a complex structure and the transitions were calorimetrically irreversible. The reversibility of denaturation was checked by comparing the first scan of the muscle fibres with the second one after cooling the sample to room temperature. The first DSC trace was corrected for the calorimetric baseline by subtracting the second scan from the first one and for the difference in heat capacity by using a linear baseline. The thermograms in strongly and weakly actin binding states could be decomposed into three to four separate transitions in the main transition temperature range (from 40 to 85°C). Using PeakFit 4.0 software from SPSS Corporation performed decomposition into four components. For analysis of the single thermal transitions Gaussian functions were assumed. The most striking feature of the traces is that the transition temperature of the last peak strongly depended on the intermediate states of the muscle (Fig. 11; Table 1).

Table 1 DSC results on muscle fibres: transition temperatures in range of 40–85°C
Glycerinated muscle fibres prepared from psoas muscle of rabbit were measured in rigor, strongly and weakly binding state of myosin to actin. The transition temperatures were derived from the original DSC curves

Experimental results	T_1/ °C	T_2/ °C	T_3/ °C	T_4/ °C
Rigor	52.2	59.2	–	67.8
ADP	53.0	57.8	–	67.8
AMP·PNP	52.7	57.7	62.1	70.4
ATP·V_i	53.6	57.8	63.3	68.9
ATP·AlF_4	52.9	57.9	64.4	74.7
ATP·BeF_x	53.2	58.4	63.8	77.8

Mean values: T_{m1}=52.9±0.7°C (n=9), T_{m2}=57.9±0.7°C (n=9), T_{m3}=63.7±1.0°C (n=7)
Slightly different values were obtained in MOPS buffer: T_{m1}=53.2±0.7°C (n=8), T_{m2}=57.3±1.0°C (n=8), T_{m3}=63.3±1.0°C (n=4)

Similar observations were obtained on isolated myosin subfragment 1 [43, 44].

Systematic analysis of irreversible denaturation of protein systems started with the model by Lumry and Eyring [45]. After this basic report several experimental studies were reported with the conclusion, that, in many cases, the irreversible denaturation of proteins by DSC can be described on the basis of a simple two-state irreversible model [46–49]. The theory assumed a reversible unfolding of the proteins that is followed by a rate-limiting irreversible step:

$$N \xrightarrow{k_{app}} F$$

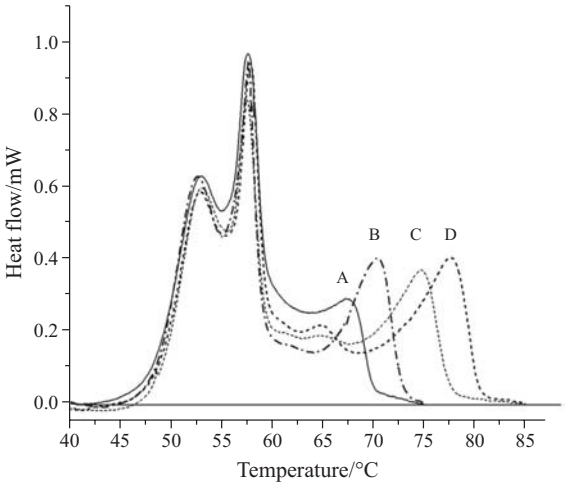

Fig. 11 DSC transition curves of muscle fibres in different intermediate states of the ATP hydrolysis. The melting temperature of the last transition depends strongly on the ligand occupied the nucleotide binding site. Symbols: A – ADP state, B – AMP·PNP state, C – ATP·AlF_4^- state, D – ATP·BeF_X^- state

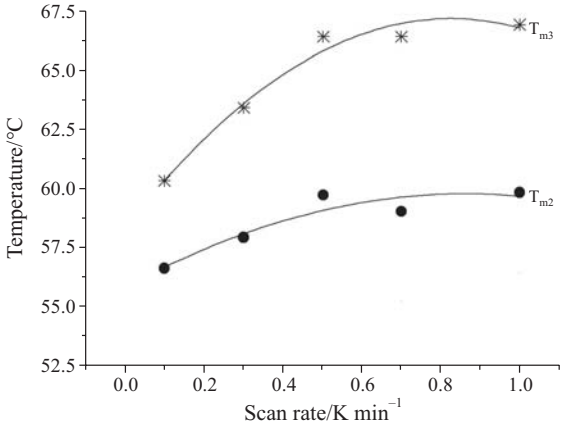

Fig. 12 Effect of scanning rate on the DSC transition temperature of glycerol-extracted muscle fibres prepared from m. psoas of rabbit. Measurements were made on fibres in rigor. Figure shows the transition temperatures of the three main transitions. Over 0.5 min K^{-1} scan rate the transition temperatures achieve approximately their limiting value

where N is the native protein; F means the final state of the irreversible denatured protein. The extent of the irreversibility is determined by the rate constant k_{app}, and its activation energy gives the rate of unfolding. The rate constant changes with temperature according to the Arrhenius equation. Recently, it was shown that in some cases the thermodynamic parameters could be deduced from the standard treatment of the heat capacity curves. It originates from the observation that the transition temperature does not depend strictly on the scan rate after a critical value of the scan rate [50], as well as the population of unfolded portion should be greater than 0.03% [51].

According to the results of muscle experiments the transition temperatures depend on scan rate, therefore it can be assumed that kinetic processes determine the melting of the muscle samples (Fig. 12). The calculation shows that $\ln\{s_r/(T_m)^2\}$ as a function of the reciprocal absolute temperature of T_m gives a straight line, where s_r is the scan rate and T_m means the transition temperature. From the plot the average activation energies could be obtained [52, 53], for the three main transitions they were 302, 636 and 328 kJ mol^{-1}, respectively. The scan rate practically reached its maximum value at about 0.5 K min^{-1}, therefore it permitted to apply a decomposition of the complex DSC patterns with Gaussian functions (Table 2). The process resulted in four transitions, the first three transition temperatures were almost independent of the intermediate state of the muscle; the last transition temperature was shifted to higher temperature, when the buffer solution was manipulated to mimic the intermediate states of ATP hydrolysis. The mean values were T_{m1}=53.2±0.7°C (n=8), T_{m2}=57.3±1.0°C (n=8), T_{m3}=63.3±1.0°C (n=4) in MOPS buffer.

Table 2 DSC results on muscle fibres: % areas of decomposed curves. Glycerinated muscle fibres prepared from psoas muscle of rabbit were measured in rigor, strongly and weakly binding state of myosin to actin. The values are the mean of three determinations. Decomposition was performed by using PeakFit 4.0 software from SPSS Corporation. For analysis of the single thermal transitions Gaussian functions were assumed. The areas of the transitions are expressed in %

Results of decomposition	T_1/ °C	T_2/ °C	T_3/ °C	T_4/ °C
Rigor	52.4	58.8	63.5	67.9
Area/%	41.2	24.6	22.9	11.4
ADP	53.2	57.6	61.5	67.1
Area/%	42.6	21.2	21.9	14.3
AMP·PNP	52.8	57.5	63.1	69.9
Area/%	42.3	23.8	12.5	21.4
ATP·V_i	54.4	57.4	63.1	69.5
Area/%	43.0	23.0	10.0	24.0
ATP·AlF_4	52.6	57.9	64.2	73.7
Area/%	35.0	23.1	19.7	22.2
ATP·BeF_x	53.3	57.8	62.9	76.9
Area/%	35.4	20.4	22.8	21.5

Application to muscle fibres in strong binding of myosin to actin

Rigor muscle

Earlier measurements performed on myosin showed that at least five endothermic transitions could be observed on bovine heart and skeletal myosin between the temperature ranges of 20–55°C [54, 55]. The highest transition temperature could be assigned to unfolding of the coiled-coil α-helix rod portion of the protein moiety [56, 57], whereas the lower transition temperature arises from melting of the head portion of the protein. The structure formation of proteins in fibres alters the dynamic and energetic properties of the proteins, the consequence of that is the shift of the melting points 39, 47 and 51°C, measured in solution on intact myosin from rabbit psoas muscle, to higher temperatures in rigor. This is evidence that particular regions of myosin are subjected to stabilizing forces in the filament system leading to alteration of the transition temperatures.

Muscle fibres in ADP state

Melting curves of glycerol-extracted muscle fibres in strong binding rigor and ADP state of myosin to actin did not exhibit large differences in Tris·HCl buffer (Fig. 13). Similar result was obtained on nucleotide-free S1 and the complex of S1 with ADP [58]. Remarkable difference between rigor and ADP state

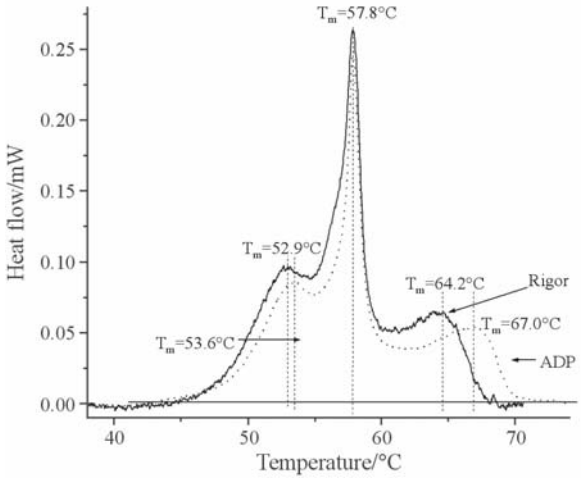

Fig. 13 DSC scans exhibit significant difference in the global conformation of strong binding rigor and ADP state

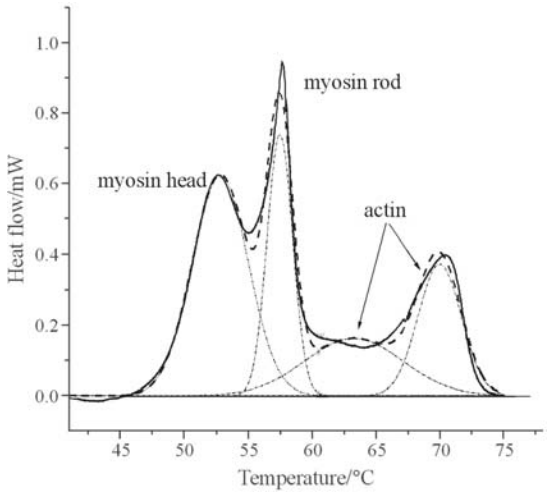

Fig. 14 Heat flow curve of muscle fibres in AMP·PNP state. Decomposition was performed by PeakFit 4.0 software. Solid line shows the original DSC transition, dashed line is the result of superposition of single transitions. Single transitions were assigned to the head of myosin, the rod of myosin and the actin

was obtained in MOPS buffer; the temperature of the last transition was shifted to higher temperature with about 3°C from 64.5 to 66.7°C.

Effect of nucleotides on thermal transitions

The comparison between the DSC patterns in different weakly binding states of myosin to actin in fibre bundles showed that the transition temperature at the first two (three) transitions varied only slightly. In contrast, the last one shifted markedly to higher temperature depending on the ternary complex, except after addition of $MgPP_i$ to rigor buffer. In the presence of $MgPP_i$ only insignificant change was detected. For direct comparison of the different states the DSC

curves were decomposed (Fig. 14). Assuming Gaussian curves for the thermal transition curves, the T_{m2} and T_{m3} transitions were subsequently subtracted from the original DSC curve. In order to obtain reasonable residuals the melting temperatures of the transitions, the contributions of the individual Gaussian curves to the total endothermic transition and their line widths at half-height of the transition temperature were varied during the manipulation.

Recently, Levitsky's group published papers that in the presence of ADP and inorganic phosphate analogues (BeF_X^-, AlF_4^- and V_i) a large shift of the transition temperature was detected during thermal unfolding of both S1 and F-actin solution [44, 48]. The transitions in muscle fibre system are due to either to the motor domain of myosin or the binding of ADP and BeF_X^- or AlF_4^- to the nucleotide-binding site of F-actin. Measurements on isolated actin showed that the melting temperature varied between 63 and 69°C, depending on the form of actin [59, 60]. Early EPR measurements on spin-labelled F-actin resulted in a T_m=67.5°C [61]. The spectral changes were reversible when the thermal treatment did not exceed 60°C. When F-actin filaments were stabilized by phalloidin or jaspakinolide, a significant increase of the transition temperature was detected [62].

In order to make a reasonable decision, differential measurements were performed. Myosin was partially extracted from one of the fibre bundles, and it was measured against an untreated fibre bundle. The masses of the fibre bundles were so adjusted that after myosin extraction the fibre bundles had equal massesin both sample holders with an accuracy of ±1 mg. The result obtained in rigor is shown in Fig. 15. Analysis of DSC trace supports the view that the last transition can be accounted for the unfolding of F-actin filaments.

Differential measurements were performed on fibre bundles as well which were differently treated before DSC measurements. Typical result is demonstrated in Fig. 16. Fibre bundles in rigor and in ADP·AlF_4^- state were denatured against each other in the same run. The main components of the fibres were affected by ATP plus AlF_4^-. The transition temperature of myosin motor shifted with about 4°C in comparison with the myosin motor in rigor, while that of the F-actin filaments increased more than 10°C. In order to interpret the DSC results we could adopt the suggestion by Hozumi and Bombardier *et al.* about the existence of a second nucleotide-binding site on F-actin [63, 64]. However, little is known about the properties and role of the second nucleotide-binding site on actin. On the other hand, Carlier *at al.* reported that phosphate release in actin was reversible; P_i could rebound to actin by producing F-actin-ADP·P_i filaments [65]. Orlova and Egelman [66, 67] have also shown by EM that beryllium fluoride and phosphate made the flexible filaments rigid, which may support an induced communication between the nucleotide binding site and other region of actin protomers. The perturbations spread to neighbouring protomers and thereby affect the dynamic nature of F-actin [68].

In both cases, the possible explanation of the DSC experiments might relay on the assumption that F-actin molecules in fibres could form two populations in the presence of nucleotides and nucleotide analogues: (*i*) protomers with MgADP or MgADP-P_i analogue in the nucleotide cleft, which distributed randomly on the

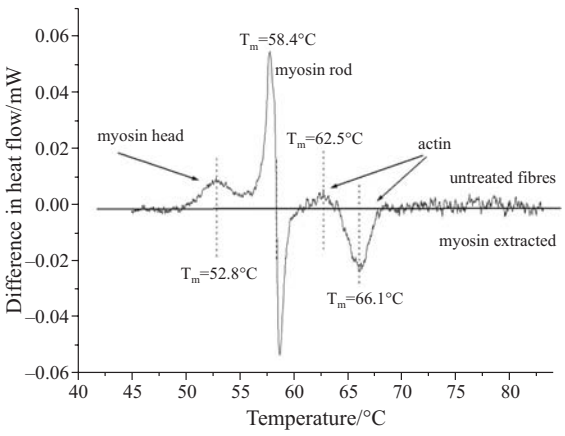

Fig. 15 Differential DSC traces of muscle fibres. Myosin was partially extracted from one of the fiber bundles, and the two fiber bundles were measured in the same run. The two samples have the sames mass; the sample after myosin extraction has relatively more actin, than the untreated sample

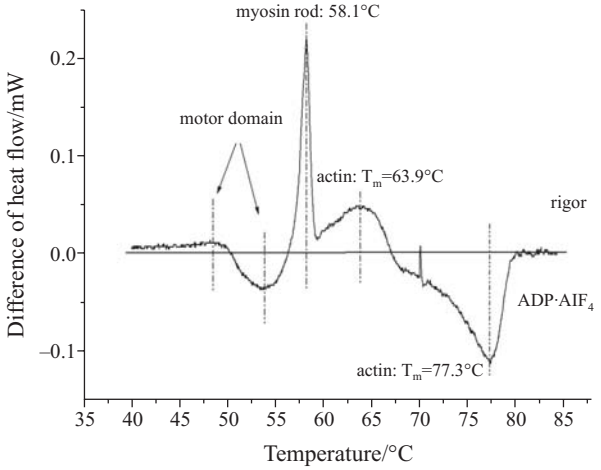

Fig. 16 Differential DSC traces of muscle fibres. The fiber bundles having the same mass were differently treated before DSC run. The large shift in ATP·BeF_X^- state originates from actin

filaments, or (*ii*) MgADP protomers in the nucleotide cleft and protomers with MgADP-P_i analogue bound to the second nucleotide binding sites, if it exists. The binding of V_i, AlF_4^- or BeF_X^- to F-actin increases the stability of filaments and leads to shift of T_{m3}. The fourth heat transition T_{m4} depended on the bound nucleotides (Table 1). The largest effect was detected in the case of BeF_X^-, and only a small effect was obtained in the presence of P_i. DSC measurements performed on F-actin solution supports the view that BeF_X^- and a lesser extent AlF_4^- stabilize F-actin, and they protect from heat denaturation [69–72].

Acknowledgements

This work was supported by grants from the National Research Foundation (OTKA CO 123, CO 272).

References

1 M. A. Geeves, Biochem. J., 274 (1990) 1.
2 K. C. Holmes, Acta Cryst., A54 (1998) 789.
3 K. C. Holmes, Nature Struct. Biol., 5 (1998) 940.
4 M. A. Geeves and K. C. Holmes, Ann. Rev. Biochem., 68 (1999) 687.
5 I. Rayment, H. M. Holden, M. Whittaker, C. B. Yohn, M. Lorenz, K. C. Holmes and R. A. Milligan, Science, 261 (1993) 58.
6 R. Dominguez, Y. Freyzon, K. M. Trybus and C. Cohen, Cell, 94 (1998) 659.
7 A. J. Fisher, C. A. Smith, J. Thoden, R. Smith, K. Sutoh, H. M. Holden and I. Rayment, Biophys. J., 68 (1995) 19.
8 A. J. Fisher, C. A. Smith, J. Thoden, R. Smith, K. Sutoh, H. M. Holden and I. Rayment, Biochemistry, 34 (1995) 8960.
9 E. Pate, N. Naber, M. Matuska, K. Franks-Skiba and R. Cooke, Biochemistry, 36 (1997) 1215.
10 C. R. Bagshaw and D. R. Trentham, Biochem. J., 141 (1974) 331.
11 T. Stone, T. Buckman, P. Nordio and H. McConnell, Proc. Natl. Acad. Sci. USA, 54 (1965) 1010.
12 D. D. Thomas, Ann. Rev. Physiol., 49 (1987) 691.
13 P. Fajer, Encyclopedia of Analytical Chemistry, R. A. Meyers, Ed., John Wiley and Sons, New York 2000.
14 P. L. Privalov and S. A. Potekhin, Methods Enzymol., 131 (1986) 4.
15 J. M. Sturtevant, Ann. Rev. Phys. Chem., 38 (1987) 463.
16 M. Zolkiewski, M. J. Redowicz, E. D. Korn and A. Ginsburg, Biophys. Chem., 59 (1996) 365.
17 D. Lőrinczy, N. Hartvig and J. Belagyi, J. Musc. Res. Cell Motil., 22 (2001) 585.
18 E. Rome, J. Mol. Biol., 65 (1972) 321.
19 D. R. Trentham, R. G. Bardsley, J. P. Eccleston and A. G. Weeds, Biochem. J., 126 (1972) 635.
20 J. G. Norby, Acta Chem. Scand., 25 (1971) 2717.
21 L. Zhao, N. Naber and R. Cook, Biophys. J., 68 (1995) 1980.
22 P. G. Fajer and D. Marsh, J. Magn. Reson., 49 (1982) 212.
23 L. Pótó, I. Frey and J. Belagyi, Abstr 11th Int. Biophys. Congr., Budapest, Hungary 1993, p. 102.
24 C. A. Evans, J. Magn. Reson., 44 (1981) 109.
25 L. I. Horváth and M. Derek, J. Magn. Reson., 54 (1983) 363.
26 C. C. Goodno, Proc. Natl. Acad. Sci. USA, 76 (1979) 2620.
27 M. M. Werber, Y. M. Peyser and A. Muhlrad, Biochemistry, 31 (1992) 7190.
28 B. C. Phan and E. Reisler, Biochemistry, 31 (1992) 4787.
29 B. C. Phan, L. D. Faller and E. Reisler, Biochemistry, 32 (1993) 7712.
30 J. Belagyi, I. Frey and L. Poto, Eur. J. Biochem., 224 (1994) 215.
31 P. G. Fajer, E. A. Fajer, J. M. Matta and D. D. Thomas, Biochemistry, 29 (1990) 5865.
32 P. G. Fajer, E. A. Fajer, N. J. Brusvold and D. D. Thomas, Biophys. J., 53 (1988) 513.
33 N. Hartvig, D. Lőrinczy, N. Farkas and J. Belagyi, Eur. J. Biochem., 269 (2002) 2168.
34 V. A. Barnett and D. D. Thomas, Biochemistry, 26 (1987) 314.
35 R. Lymn and E. W. Taylor, Biochemistry, 10 (1971) 4617.
36 D. R. Trentham, J. P. Eccleston and C. R. Bagshaw, Q. Rev. Biophys., 9 (1976) 217.
37 K. A. Johnson and E. W. Taylor, Biochemistry, 17 (1978) 3432.
38 J. A. Danzig and Y. E. Goldman, J. Gen. Physiol., 86 (1985) 305.
39 S. Maruta, G. D. Henry, B. D. Snykes and M. Ikebe, J. Biol. Chem., 268 (1993) 7093.
40 A. M. Gulick, C. B. Bauer, J. B. Thoden and I. Rayment, Biochemistry, 36 (1997) 11619.
41 B. Brenner, T. Kraft and L. C. Yu, Biophys. J., 53 (1988) 24a.
42 T. Kraft, L. C. Yu, H. J. Kuhn and B. Brenner, Proc. Natl. Acad. Sci. USA, 89 (1992) 11362.
43 D. Lőrinczy and J. Belagyi, Biophys. Biochem. Res. Commun., 217 (1995) 592.
44 D. Lőrinczy, The nature of biological systems as revealed by thermal analysis, D. Lõrinczy, Ed., Kluwer Acad. Publisher, Dordrecht 2004, pp. 159–186.
45 R. Lumry and H. Eyring, J. Phys. Chem., 58 (1954) 110.
46 J. M. Sanchez-Ruiz, J. L. Lopez-Lacomba, M. Cortijo and P. L. Mateo, Biochemistry, 27 (1988) 1648.
47 F. Conjero-Lara, P. L. Mateo, F. X. Aviles and J. M. Sanchez-Ruiz, Biochemistry, 30 (1991) 2067.
48 M. Thorolfsson, B. Ibarra-Molero, P. Fojan, S. B. Petersen, J. M. Sanchez-Ruiz and A. Martinez, Biochemistry, 41 (2002) 7573.
49 M. L. Galisteo, P. L. Mateo and J. M. Sanchez-Ruiz, Biochemistry, 30 (1991) 2061.
50 T. Vogl, C. Jatzke, H-J. Hinz, J. Benz and R. Huber, Biochemistry, 36 (1997) 1657.
51 G. D. Manetto, C. La Rosa, D. M. Grasso and D. Milardi, J. Therm. Anal. Cal., 80 (2005) 263.
52 B. Bugyi, G. Papp, Sz. Halasi and B. Visegrády, J. Therm. Anal. Cal., 82 (2005) 275.
53 G. Papp, B. Bugyi, Z. Ujfalusi, Sz. Halasi and J. Orbán, J. Therm. Anal. Cal., 82 (2005) 281.
54 K. Samejima, M. Ishioroshi and T. Yashui, Agric. Biol. Chem., 47 (1983) 2373.

55 D. Lőrinczy, U. Hoffmann, L. Pótó, J. Belagyi and P. Laggner, Gen. Physiol. Biophys., 9 (1990) 589.
56 M. Zolkiewski, M. J. Redowicz, E. D. Korn and A. Ginsburg, Biophys. Chem., 59 (1996) 365.
57 A. Bertazzon and T. Y. Tsong, Biochemistry, 29 (1990) 6453.
58 D. I. Levitsky, O. P. Nikolaeva, V. N. Orlov, D. A. Pavlov, M. A. Ponomarev and E. V. Rostkova, Biochemistry (Moscow), 63 (1998) 381.
59 A. Bertazzon and T. Y. Tsong, Biochemistry, 29 (1990) 6447.
60 D. Lőrinczy, F. Könczöl, B. Gaszner and J. Belagyi, Thermochim. Acta, 322 (1998) 95.
61 J. Belagyi, W. Damerau and G. Pallai, Acta Biochim. Biopyhs. Acad. Sci. Hung., 13 (1978) 85.
62 B. Visegrády, D. Lőrinczy, G. Hild, B. Somogyi and M. Nyitrai, FEBS Letter, 565 (2004) 163.
63 T. Hozumi, J. Biochem., 104 (1988) 285.
64 H. Bombardier, P. Wong and C. Gicquaud, Biochem. Biophys. Res. Comm., 236 (1997) 798.
65 M.-F. Carlier and D. Pantaloni, J. Biol. Chem., 263 (1988) 817.
66 A. Orlova and E. H. Egelman, J. Mol. Biol., 232 (1993) 334.
67 A. Orlova and E. H. Egelman, J. Mol. Biol., 227 (1992) 1043.
68 A. Muhlrad, P. Cheung, B. C. Phan, C. Miller and E. Reisler, J. Biol. Chem., 269 (1994) 11852.
69 C. Combeau and M-F. Carlier, J. Biol. Chem., 263 (1988) 17429.
70 P. Dancker and G. H. Schmied, Z. Naturforsch., 44c (1989) 698.
71 T. Dergez, F. Könczöl, N. Farkas, J. Belagyi and D. Lőrinczy, J. Therm. Anal. Cal., 80 (2005) 445.
72 J. Orbán, K. Pozsonyi, K. Szarka, Sz. Barkó, E. Bódis and D. Lőrinczy, J. Therm. Anal. Cal., 84 (2006) 619.

Received: June 12, 2006
Accepted: December 29, 2006
OnlineFirst: February 26, 2007

DOI: 10.1007/s10973-006-7728-6